DEHAZING USING LIFTING WAVELET AND LAPLACIAN MATTE

A PROJECT REPORT

Submitted by

PRABH PREET SINGH

2K13/SPD/24

in partial fulfillment for the award of the degree of

MASTER OF TECHNOLOGY

in

SIGNAL PROCESSING AND DIGITAL DESIGN

under the supervision of

DR. SUDIPTA MAJUMDAR

ASSISTANT PROFESSOR

DEPARTMENT OF

ELECTRONICS & COMMUNICATION ENGINEERING

DELHI TECHNOLOGICAL UNIVERSITY

DELHI

(BATCH: 2013-2016)

DECLARATION

I hereby state that the work which is being presented in the thesis report entitled **DEHAZING USING LIFTING WAVELET AND LAPLACIAN MATTE** by **Prabh Preet Singh** in partial fulfillment of requirements for the award of degree of **Master of Technology in Signal Processing and Digital Design** submitted at **Department of Electronics and Communication Engineering, Delhi Technological University, New Delhi** is an authentic record of my own work. The matter presented in this thesis report has not been submitted by me in any other University / Institute for the award of Mater of Technology degree.

Prabh Preet Singh
Enrollment No.: 2K13/SPD/24

July, 2016

DELHI TECHNOLOGICAL UNIVERSITY

CERTIFICATE

This is to certify that the thesis entitled **DEHAZING USING LIFTING WAVELET AND LAPLACIAN MATTE** submitted by **Prabh Preet Singh**, enrollment number **2K13/SPD/24** at **Department of Electronics and Communication Engineering, Delhi Technological University, Delhi** for partial fulfillment of requirements for the award of degree of **Master of Technology in Signal Processing and Digital Design** has been carried out by him under my supervision.

Dr. Sudipta Majumdar
Assistant Professor
Department of Electronics and Communication Engineering
Delhi Technology University
New Delhi - 110042

July, 2016

ACKNOWLEDGEMENT

I would like to express my gratitude to my supervisor Dr. Sudipta Majumdar for the useful comments, remarks and engagement throughout the learning process of this master thesis.

Furthermore I would like to thank Mr. Rajesh Rohilla and our Head of Department, Mr. Prem R. Chaddha for the support on the way.

Also, I would like to thank my line manager at Nokia, Sandeep Arora and Chiranjeev Singh (IIM-A grad.) for kind support during the course of this research. I would like to thank my loved ones, who have supported me throughout entire process.

ABSTRACT

This work presents single image dehazing based on dark channel prior. Firstly, lifting haar wavelet has been used to decompose the hazy image into approximation and details. Then only the approximation component which is just one-fourth of the actual image dimension is further processed for dehazing. The dark channel prior used in the proposed work for dehazing is based on statistics of haze free images. The property that the intensity of dark channel gives approximate thickness of the haze is used to estimate the transmission and atmospheric light. Instead of constant airlight, proposed method employs scene depth to estimate spatially varying atmospheric light as it truly occurs in nature. Haze imaging model together with soft matting method has been used in this work to obtain a high quality haze free image. Experimental results demonstrate that the proposed approach produces better results as color fidelity and contrast of haze free image are improved and no over saturation in the sky region is observed. Further, with the use of lifting wavelet transform, reduction in computational time by a factor of two to three as compared to the conventional approach has been observed.

CONTENTS

CHAPTER 1

INTRODUCTION

While the whole world unites to curb air pollution that poses a serious threat to our environment, we focus to work on another phenomenon caused by air pollution called haze. Haze is an atmospheric phenomenon that degrades visual quality of an image thereby affecting the performance of many computer vision applications. Haze removal is a difficult task because thickness of haze depends upon depth, which is unknown. To estimate depth from a single image is an under constrained problem. Therefore many methods exist which are based upon multiple images or some additional information. Since in many real applications, obtaining multiple images of the same scene is not possible, single image dehazing has gained popularity. The success of various single image dehazing techniques depends on the accuracy and generality of their priors/ assumptions.

Recently, in single image dehazing, Dark Channel Prior, proposed by He et al. [1], has gained popularity because of its simplicity and effectiveness to remove haze in most of the cases. DCP depends on the perception that in a large portion of the outdoor haze free images, no less than one color channel has negligible intensity in a patch. Though effective, DCP fails in sky regions and in case of near white objects. Moreover, due to solving of laplacian matte, DCP is computationally intensive.

In this work, we propose an approach, partly derived from some of the previously developed methodologies, to make DCP suitable for real time applications and at the same time ensuring high visual quality output. We apply lifting Haar wavelet decomposition to reduce computation runtime and memory requirement. We also apply depth based atmospheric light to estimate it correctly even in the presence of Sun or any other light source which form the reason for non-uniform airlight.

1.1 Thesis Overview

This report is organized in following manner. In chapter 2, we discuss haze imaging model which is the baseline of our entire discussion and discuss our comprehensive study on various dehazing techniques built upon dark channel prior assumption. In chapter 3, we thoroughly review dark channel prior approach proposed by He et al. [1]. In chapter 4, we discuss the scenarios where the classical dark channel prior fails and propose methodology to eliminate the limitations. Further, we present our end to end algorithm for image dehazing. In chapter 5, we summarize results and simulations. Also, we present comparative study between our method and state-of-the-art DCP technique. In chapter 6, we conclude our work followed by future scope of work in chapter 7.

CHAPTER 2

BACKGROUND

In this chapter, the first section presents Haze Imaging Model described by a mathematical equation. This model forms the basis for our thesis and has been used extensively in the report.

The later section discusses the previous works on single image haze removal based on He's [1] Dark Channel Prior. Accordingly the performance and limitations of the stated works has been commented as evaluated during the course of our study.

2.1 Haze Imaging Model

In 1975, McCartney proposed airlight scattering model [2]. Later, Narasimhan and Nayar [3] further simplified it. The haze imaging model, which is now widely used in image processing is:

$$I(x) = t(x)J(x) + A(1 - t(x)) \tag{2.1}$$

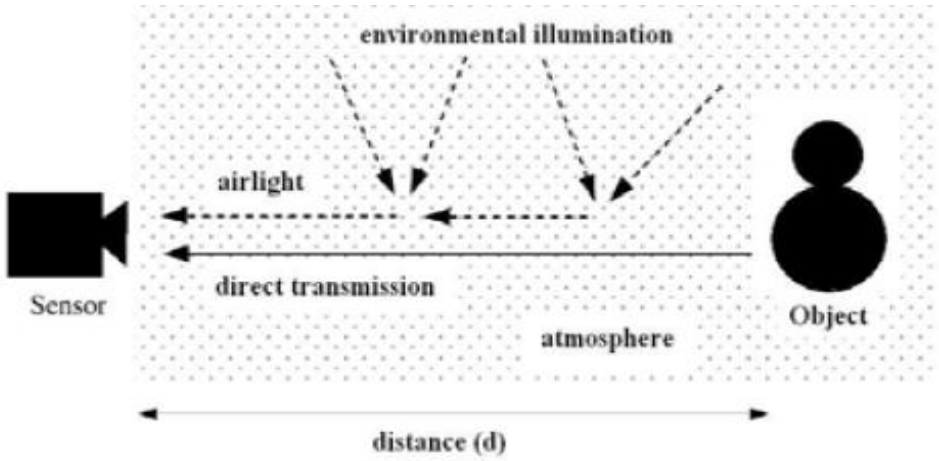

Figure 2.1: Haze Imaging Model [3]

where,

'x' denotes the position of the pixel in the image

'I' denotes the observed hazy image intensity

'J' denotes the scene radiance

'A' is the atmospheric light. It is a 3D RGB vector that represents the color of the atmosphere or sky

't' is transmission of the medium associated with the portion of light reaching the camera. Now, suppose that a point in an image is situated at a distance 'd' from the camera or in other words, it has depth 'd', then, the relation between transmission and depth is given by the equation below:

$$t(x) = e^{-\beta d(x)} \tag{2.2}$$

where, $'\beta'$ is known as the 'scattering coefficient'.

Due to finite transmission of the medium, light reaching the camera directly from the object undergoes attenuation. This is expressed by the first term in (2.1) i.e. 'J(x) t(x)'.

This is termed as *'direct attenuation'*. This distortion to the scene radiance is multiplicative in nature as can be seen from the equation.

Light reaching the camera not directly from the object but due to scattering from the particles present in the atmosphere is called *'airlight'*. This distortion to scene radiance is additive in nature and is expressed by the second term in (2.1) i.e. 'A (1 - t(x))'.

2.2 Literature Survey

Various researches have been built upon He's Dark Channel Prior assumption. Some of those techniques are studied and investigated as below.

Yogesh et al. [4] used erosion and dilation to replace soft matting. Their technique is capable of removing halo to some extend for patch no larger than 3x3 and that too with oversaturation of image as a tradeoff.

Cheng-Hsiung Hsieh et al. [5] proposed dual dark channel approach with 1x1 and 15x15 patch to eliminate soft matting refinement, however it suffers from halos in depth discontinuities.

Jiajie Liu et al. [6] aimed to accurately estimate the transmission based on distance between pixel intensity and atmospheric light. While it works well for sky region, performance is not satisfactory for purely non-sky images.

Chia-Hung Yeh1 et al. [7] introduced bright channel prior as contrary to dark channel prior to identify the regions having minimum haze thickness. This prior fails due to the presence of black objects and shadow areas in most of the images. As per our study, we propose to determine minimum haze regions corresponding to the darkest pixels in the dark channel instead.

For sky regions, dark channel of haze free image is not zero. He [1] assumed it zero when calculating transmission that leads to oversaturation in sky regions. Xipan Lu et

al. [8] tried to rectify this issue by introducing an adaptive compensation in transmission computation that varies for sky and non-sky regions accordingly.

To deal with sky region, Ting Han and Yi Wan [9] modified transmission according to the difference between pixel intensity and atmospheric light. The proposed technique works well for the sky region but oversaturates rest of the image. When tuned for the non-sky region, it does not work well for the sky part, so it is tough to find parameters that suit sky and non-sky regions simultaneously.

Hung-Yu Yang et al. [10] employed median filter as a refinement algorithm replacing soft matting for underwater image enhancement and is computationally very efficient to do so. However, it causes great loss to the color fidelity of the recovered image.

Yanjing Yang et al. [11] speeded up the algorithm by processing only the low frequency sub-image obtained using discrete Haar wavelet transform.

C. Chengtao et al. [12] segmented the hazy image into sky and non-sky regions and processed them separately to resolve the problem of dimness and oversaturation. The threshold segmentation employed here requires manual tuning as optimum threshold value may vary from image to image.

There are many techniques deploying pixel based dark channel prior. Though it avoids any refinement process to remove halos and blocky artifacts, it cannot take care of white objects such as cars etc. Firstly, this leads to inaccurate estimation of atmospheric light. Secondly, dark channel of white objects is not dark causing underestimation of transmission. Both of the cases lead to oversaturation of haze free images.

CHAPTER 3

DARK CHANNEL PRIOR BASED SINGLE IMAGE HAZE REMOVAL

Our aim is to recover haze free image i.e. scene radiance. With reference to haze imaging equation (2.1) introduced in previous chapter, we need to find atmospheric light ‘A’ and transmission ‘t’ to recover the scene radiance ‘J’ for a given hazy image ’I’. It can be observed from the equation, for an image consisting of ‘N’ pixels, there will be 3N constraints and 4N + 3 unknowns. Therefore, the problem of single image dehazing is highly under constrained.

This chapter discusses Dark Channel Prior algorithm proposed by He et al. [1].

3.1 Dark Channel Prior

Knowing image dehazing model is an ambiguous problem, two strategies are available:

1. Multiple image dehazing and

2. Single image dehazing.

Multiple images of same scene under different conditions being not very practical, single image dehazing techniques are favorable. But due to ambiguity involved, assumptions or a priori knowledge is requisite.

Tan's method [13] is based on the assumption that the contrast of the haze free images is more than the hazy image. This method though gives visually appealing results, it does not well maintain the color fidelity.

Fattal [14] proposed that the luminance and transmission are independent statistically. Though effective, but the method fails for the thick haze regions.

In the method proposed by He et al. [1], it is assumed that in a large portion of the outdoor haze free images, no less than one color channel has negligible intensity in a patch. He named this assumption as "Dark Channel Prior". The prior can be easily validated from the observations below:

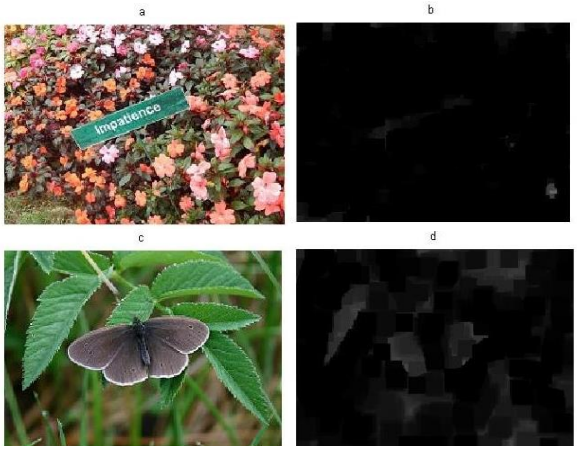

Figure 3.1: (a & c) Haze free images; (b & d) corresponding dark channels

Factors that contribute to the validity of this prior are colorful objects, shadows, irregular geometry, black objects etc. This condition is valid only for haze free images except where sky region or near white objects come into picture.

For hazy images, dark channel is not really dark as shown below. This is so because addition of the airlight causes brightening of the pixels which are otherwise dark for

haze free image. The thicker the haze more is the extent of brightness. This distinction allows using the prior for dehazing purpose.

Figure 3.2: (a & c) Haze free images; (b & d) corresponding dark channels

3.2 Haze Removal Algorithm

Steps involved in the classical DCP algorithm are shown in the block diagram:

Figure 3.3: Block Diagram for Classical DCP Algorithm

3.3 Dark Channel Computation

To evaluate dark channel for an image, a window or patch of size 15 x 15 is moved over the whole image. Dark channel for the pixel at the center of the window is equal to the minimum intensity value among the three color channels, i.e. Red, Green and Blue, and

among all the pixels in that patch. Mathematically, the dark channel of an image can be expressed as:

$$I^{dark}(x) = \min_{y \in \Omega(x)} \left(\min_{c \in \{R,G,B\}} I^{c}(y) \right) \tag{3.1}$$

where, Ω denotes the patch of 15 x 15 pixels and c denotes the color channel.

3.4 Atmospheric Light Estimation

Intuitively, the pixels representing the atmospheric light can be thought of as the brightest pixels. But this simple definition goes wrong when some white objects like white car or white building is present in the image. In this case the white object will have the brightest pixels but it is obviously not the airlight. The definition will also fail easily in the presence of sunlight which cannot be ignored in most of the outdoor images.

For more accurate results, He et al. [1] make use of dark channel of the image. The dark channel depicts the thickness of haze and thus can be used for estimation of airlight. As dark channel is calculated in a patch, the white objects which are generally surrounded by colored objects become dark in dark channel image. Thus, the brightest pixels in the dark channel image are not the bright or white objects in the hazy image. Therefore, airlight now can be accurately estimated from the dark channel. He et al. [1] estimate atmospheric light as the average of the pixel intensities in the hazy image corresponding to 0.1 % of the bright pixels in the dark channel. Note that He et al. [1] considers atmospheric light ‘A’ to be constant over the whole image.

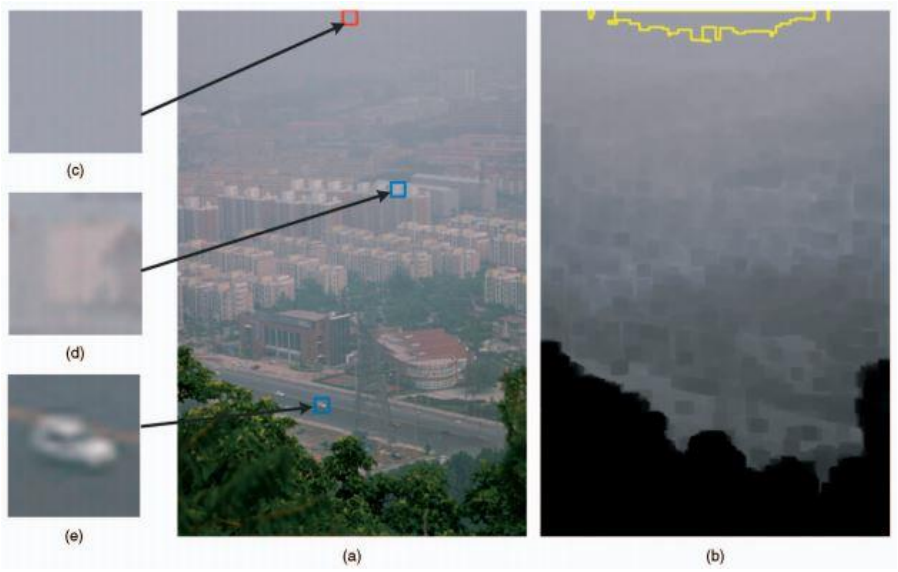

Figure 3.4: (a) Hazy Image (b) Corresponding Dark Channel (c) Brightest pixels in the dark chaneel (d) & (e) shows the brightest pixel in the hazy image [1]

3.5 Transmission Estimation

Given atmospheric light A as calculated above and assuming that the transmission in a local patch is constant, we can estimate the transmission using haze imaging equation (2.1):

$$I(x) = t(x)J(x) + A(1 - t(x)) \tag{2.1}$$

Normalizing the haze imaging equation by atmospheric light A for each color channel independently, we get:

$$\frac{I^c(x)}{A^c} = t(x)\frac{J^c(x)}{A^c} + 1 - t(x) \tag{3.2}$$

We calculate the dark channel of either sides of equation (3.2) with an assumption that transmission remains constant in patch $\Omega(x)$. Putting minimum operator on both sides, we get,

$$\min_{y\in\Omega(x)}\left(\min_{c}\frac{I^c(x)}{A^c}\right)=\tilde{t}(x)\min_{y\in\Omega(x)}\left(\min_{c}\left(\frac{J^c(x)}{A^c}+(1-t(x))\right)\right) \tag{3.3}$$

Here, $\tilde{t}(x)$ denotes transmission in a patch. Since transmission, $\tilde{t}(x)$ is constant for a patch it can be taken out of the minimum operator. Next, as observed in the previous section (3.1) the dark channel of haze free image or correspondingly the scene radiance J is close to zero. Thus we can write:

$$J^{dark}(x)=\min_{y\in\Omega(x)}(\min_{c}J^c(y))=0 \tag{3.4}$$

This also implies that:

$$\min_{y\in\Omega(x)}\left(\min_{c}\frac{J^c(x)}{A^c}\right)=0 \tag{3.5}$$

Substituting equation (3.5) in equation (3.3), we get,

$$\tilde{t}(x)=1-\min_{y\in\Omega(x)}\left(\min_{c}\frac{I^c(x)}{A^c}\right) \tag{3.6}$$

3.6 Soft Matting

Since the transmission is assumed to be constant in a patch of size 15 x 15, there appear blocky artifacts and halos in the processed image. To deal with this problem, He et al. [1] employed soft matting proposed by A. Levin et al. [15] to refine the transmission and hence the scene radiance.

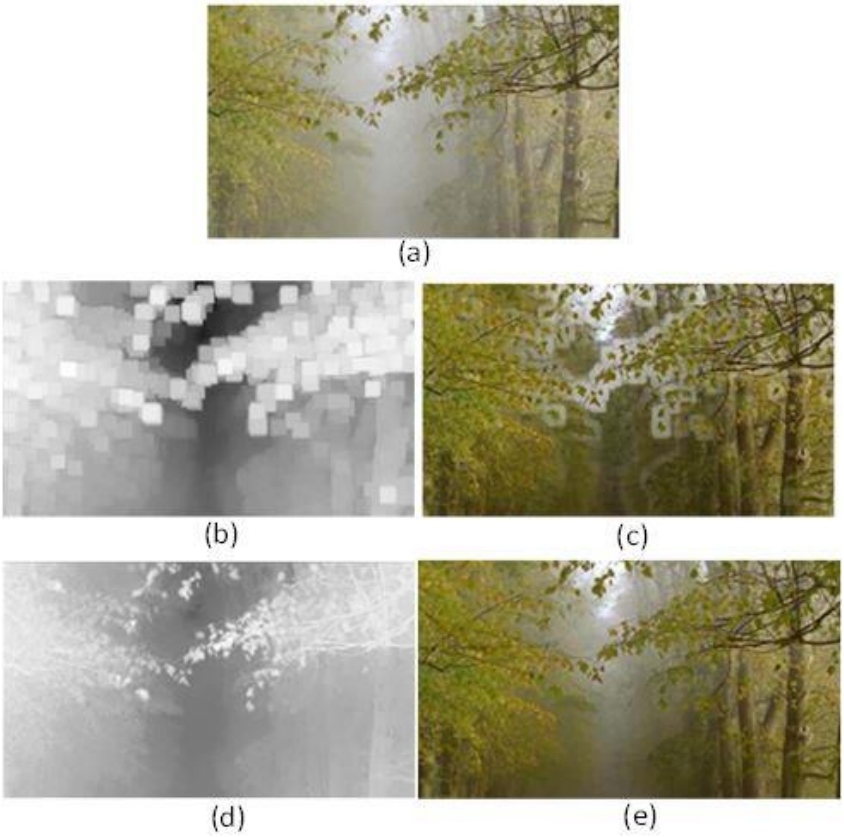

Figure 3.5: (a) Hazy Image, (b) Transmission with 15x15patch, (c) Recovered Haze free image, (d) Transmission after soft matting, (e) Recovered Haze free image after soft matting [1]

The refined transmission t is obtained from the coarse transmission $\tilde{t}$ by minimizing the following cost function:

$$E(t) = t^T L t + \lambda (t - \tilde{t})^T (t - \tilde{t}) \tag{3.7}$$

where λ is the weight and L is $N \times N$ laplacian matrix whose (i, j)th element is given by:

$$\sum_{k|(i,j)\epsilon\omega_k} \left(\delta_{ij} - \frac{1}{|\omega_k|} \left(1 + (I_i - \mu_k)^T \left(\Sigma_k + \frac{\varepsilon}{|\omega_k|} U_3 \right)^{-1} (I_j - \mu_k) \right) \right) \tag{3.8}$$

where,

I_i and I_j : colors of the input image I at pixels i and j,

δ_{ij} : Kronecker delta, μ_k : mean matrix of colors in the window ω_k,

Σ_k : covariance matrix of colors in the window ω_k,

U_3 : 3x3 identity matrix, : regularizing parameter,

$|\omega_k|$: number of pixels in the window ω_k.

Optimum value of t is obtained by solving the following equation:

$$(L + \lambda U)t = \lambda \tilde{t} \tag{3.9}$$

Where U is an identity matrix of size N x N and λ is the weight set to 10^{-4}

As observed from the figure above, recovered image obtained after soft matting is free from blocky artifacts and halo effects.

3.7 Recovering Scene Radiance

Having estimated the transmission and atmospheric light, scene radiance can be calculated using the haze imaging model. However, the transmission can be very low for pixels resembling the atmospheric light. For very low transmission values, the scene radiance will be highly amplified leading to color distortion. To avoid this situation, He et al. [1] put a lower limit on t i.e. $t0$ which is kept as 0.1. Mathematically,

$$J(x) = \left(\frac{I(x) - A}{max(t(x), t_0)} \right) + A \tag{3.10}$$

CHAPTER 4

PROPOSED METHOD

In this chapter, we propose our algorithm discussing the shortcomings of classical DCP and providing solutions to overcome them.

4.1 Accelerate Using Lifting Wavelets

When viewed in frequency domain, haze is low frequency noise. So, to eliminate haze from an image, we may just process the low frequency component of image instead of processing the whole image. This leads to drastic reduction in run time of the dehazing algorithm.

Yanjing Yang et al. [11], employed Haar discrete wavelet transform for image dehazing.

We employ lifting Haar wavelet to decompose hazy image into four sub images. Out of these four, one image contains the low frequency components i.e. it contains haze. So,

we process further only this low frequency sub image for haze removal. This makes our algorithm fast.

4.1.1 The Lifting Scheme

First generation wavelets are translation and dilation of some function. Traditionally, they are implemented using filter banks and decimators. Lifting scheme, developed by Wim Sweldens[16]-[19], gives freedom to implement or construct a wavelet, which is not necessarily translation and dilation of any function, i.e., second generation wavelets. Lifting converts traditional filter bank based implementation of discrete wavelet transform to finite and simple steps. It starts with splitting the sequence into odd and even, which is termed as Lazy wavelet transform. This transform has no function as such but forms the basis on which more sophisticated wavelet with enhanced properties is built. Lifting steps are composed of prediction and error in each stage. While scaling coefficients become the input data sequence to the next stage, wavelet coefficients are the difference in odd sample sequence and its prediction, i.e., prediction error. The simple steps of lifting are a benediction of similarities between the high pass and low pass filters used in filter bank implementation. This exploitation of similarities renders the speed to the lifting algorithm. The detail mathematical derivation for these is given in appendix section.

Lifting scheme can be illustrated by diagram below:

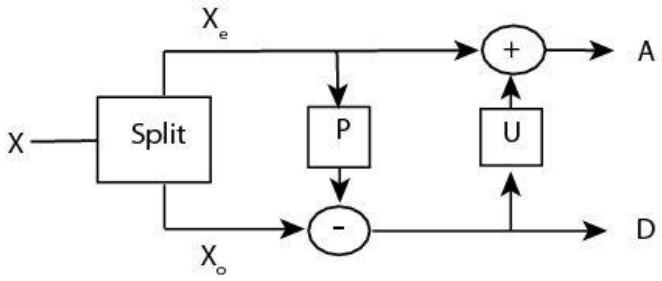

Figure 4.1: Lifting scheme implementation [27]

As shown in the figure, Lifting involves three simple steps: Split, Predict and Update, which are discussed below:

Split: This step divides the data stream 'x' into even and odd parts.

$$x_e(n): x(2n); \qquad x_o(n): x(2n+1) \tag{4.1}$$

Predict: This step predicts the next odd value from the even value. In case of Haar, the prediction is an identity function, i.e. the prediction is the even value itself. The predictions when subtracted from odd values give detail coefficients.

$$x_o(n) = P\big(x_e(n)\big) + d(n) \tag{4.2}$$

Update: To maintain the average of the input, in the update step, the even stream is updated using odd values. In case of Haar wavelets, the updating step reduces to subtracting half of the details from even values.

$$a(n) = x(2n) + U(d(n)) = (x(2n) + x(2n+1))/2 \tag{4.4}$$

Lifting scheme bear several benefits as given below:

- Less computation speed and complexity
- In place algorithm, i.e., does not require axillary memory
- Makes implementation of integer to integer transform easy
- Inverse lifting transform easily follows simply by reversing the order and sign
- Enable to construct second generation wavelets.

4.1.2 Haar wavelet decomposition into Lifting

Haar transform has 2 filter coefficients:

Low pass

$$h_0 = h_1 = 1 \tag{4.5}$$

High pass

$$g_0 = -\frac{1}{2}, \quad g_1 = h_1 = \frac{1}{2} \tag{4.6}$$

Using filter coefficients in equations A.25 to A.30 in appendix, $P(z)$ can be decomposed to

$$P(z) = \begin{bmatrix} h_e(z) & g_e(z) \\ h_o(z) & g_o(z) \end{bmatrix} = \begin{bmatrix} 1 & -\frac{1}{2} \\ 1 & \frac{1}{2} \end{bmatrix} = \begin{bmatrix} 1 & 0 \\ 1 & 1 \end{bmatrix} \begin{bmatrix} 1 & -\frac{1}{2} \\ 0 & 1 \end{bmatrix} \tag{4.7}$$

Approximate and detail coefficients can be obtained from the relation:

$$\begin{bmatrix} \lambda(z) \\ \gamma(z) \end{bmatrix} = P(z)^{-1} \begin{bmatrix} f_e(z) \\ z^{-1} f_o(z) \end{bmatrix} \tag{A.17}$$

where

$$P(z)^{-1} = \begin{bmatrix} 1 & \frac{1}{2} \\ 0 & 1 \end{bmatrix} \begin{bmatrix} 1 & 0 \\ -1 & 1 \end{bmatrix} \tag{4.8}$$

After normalization, we get

$$P(z)^{-1} = \begin{bmatrix} \sqrt{2} & 0 \\ 0 & \frac{1}{\sqrt{2}} \end{bmatrix} \begin{bmatrix} 1 & \frac{1}{2} \\ 0 & 1 \end{bmatrix} \begin{bmatrix} 1 & 0 \\ -1 & 1 \end{bmatrix} \tag{4.9}$$

4.1.3 Lifting in 2D

The block diagrams representing implementation of discrete wavelet transform using traditional filter bank technique and the lifting scheme are shown below. As can be easily observed, lifting involves simple operations whereas filter bank implementation involves complex operations of convolution, decimation and interpolation.

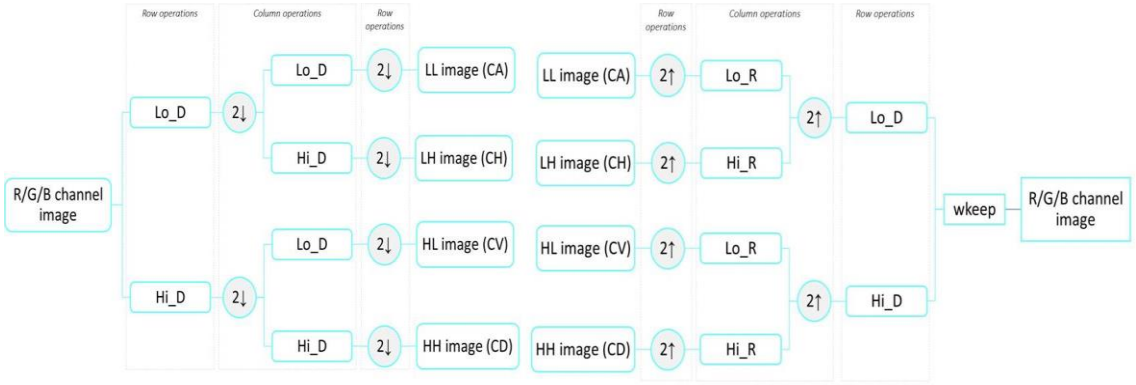

Figure 4.2: DWT and IDWT Block Diagram

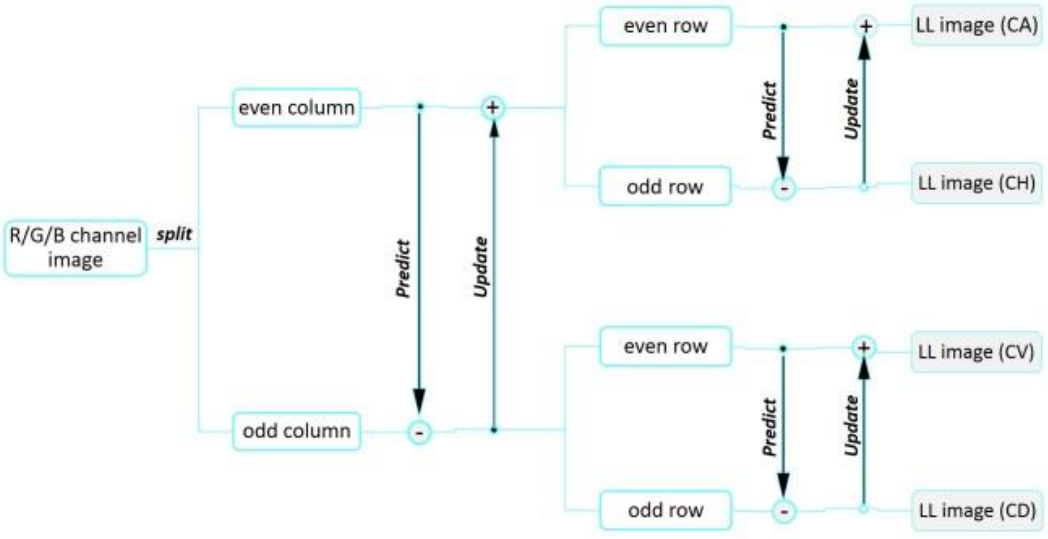

Figure 4.3: Block diagram showing lifting wavelet scheme implementation for images

Figure 4.5 illustrates the four components of the image shown in figure 4.4 obtained subsequent to wavelet decomposition. The approximation image contains the haze component and is the one which need to be further processed by dehazing algorithm.

Figure 4.4: Hazy image

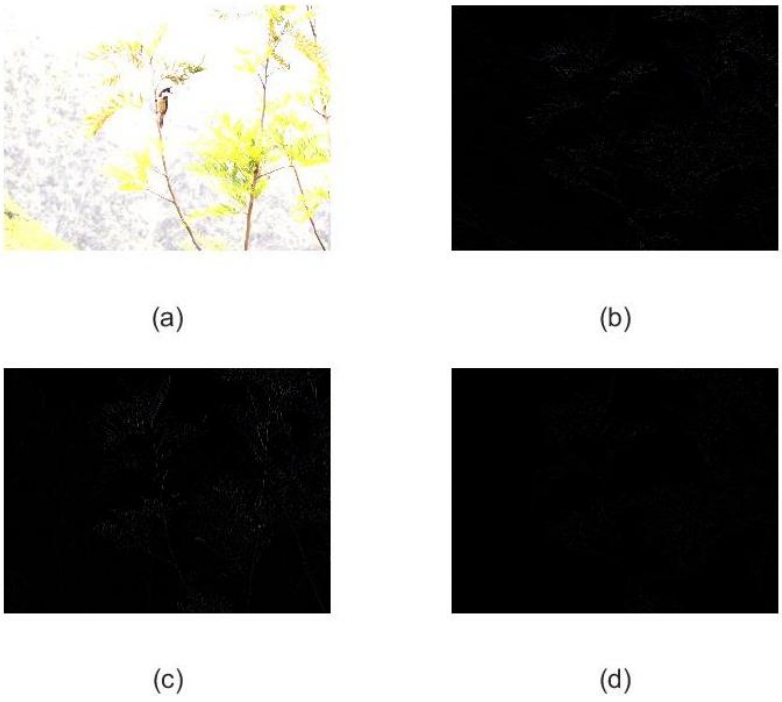

Figure 4.5: Wavelet decomposition (a) Approximation image (b) Horizontal details (c) Vertical details (d) Diagonal details

4.2 Computing Dark Channel Prior

In our algorithm, dark channel of an image is computed using the formula given below employing patch size of 15 x 15.

$$I^{dark}(x) = \min_{y \in \Omega(x)} \left(\min_{c \in \{R,G,B\}} I^c(y) \right) \tag{3.1}$$

Following figure shows hazy image and its corresponding dark channel:

Figure 4.6: (a) Hazy image (b) Corresponding dark channel

4.3 Optimizing Atmospheric Light Estimation

In method proposed by He et al. [1], atmospheric light is assumed to be constant throughout the image. This is not true because:

1) Haze density is different for different image regions and therefore atmospheric light should also vary accordingly.
2) Due to the presence of sky region or say sunlight, atmospheric light is more in one part of the image than other.

3) When localized light sources are present in the image like street light, vehicle headlights, and lamps etc., atmospheric light is more near the center of these sources.

Thus, ‘A’ is not constant. The impact of keeping ‘A’ constant can be seen in the figure below:

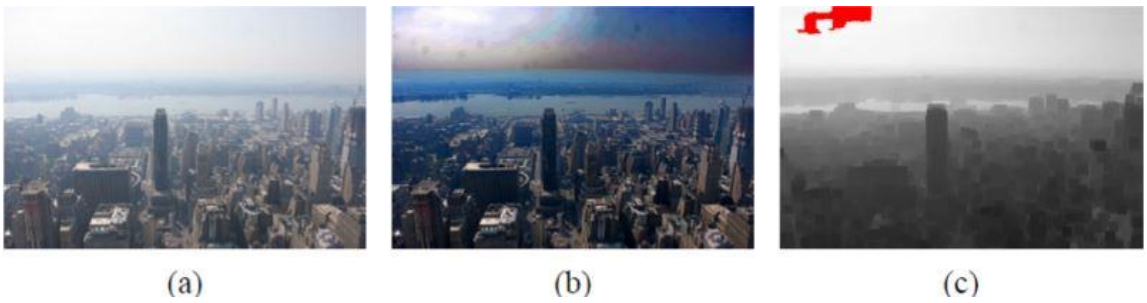

Figure 4.7: Nonconstant atmospheric light (a) Input image (b) He's result (c) Dark Channel. Red pixels indicate where the atmospheric light is estimated [1]

As we observe, sky is oversaturated. This is because the atmospheric light is measured from the region near the light source because it is here where we get brightest pixels in the dark channel. Now, this airlight is kept constant to solve the image dehazing model. Though it works correctly near the light source, the airlight is overestimated for the rest of the image. As a result, the transmission which is calculated from atmosphere, is underestimated, this in turn leads to overestimation of recovered scene radiance.

C. Chengtao et al. [12] segmented the image into sky and non-sky regions, using threshold based segmentation, and then calculated separately the critical parameters like atmosphere and transmission. The method required manual tuning of threshold value for different images.

Chia – Hung Yeh et al. [7] formulates the expression for calculating atmospheric light at every pixel. The formula is based on the fact that atmospheric light is directly proportional to haze thickness. They estimate the haze thickness by finding the difference of every pixel in the image from the brightest pixel in HSV color space. Lesser the difference more is the thickness of haze. Then the parameter is converted such as it becomes directly proportional to haze thickness. This is finally multiplied to

constant atmospheric light to make it vary according to haze. Though the idea seems to be impressive, the metric chosen for estimating haze thickness fail in case of near white objects present in the scene for which the difference from the brightest pixel is low even when they are under thickest haze.

In our proposed method, we estimate pixel based atmospheric light from scene depth. The idea is that more the scene depth more is the thickness of haze and more is the atmospheric light. Depth is estimated from the transmission using equation (2.2):

$$t(x) = e^{-\beta d(x)} \tag{2.2}$$

where, β is the scattering coefficient. Equation (2.2) can be rewritten as:

$$d(x) = \frac{1}{\beta} \ln\left(\frac{1}{t(x)}\right) \tag{4.10}$$

Based on this depth value, constant value of atmosphere is varied across the image using the expression below:

$$A \propto 1 - e^{-depth} \tag{4.11}$$

Proposed method is capable of working for varying sizes of light sources; it does not require manual tuning and also works correctly for near white scenes.

The atmospheric light calculated by the proposed method is depicted below:

(a) (b)

Figure 4.8: (a) Hazy iamge (b) Atmospheric light calculated using proposed method

4.4 Optimizing Transmission Estimation

In proposed method, transmission is estimated using haze imaging model with the only difference that now atmospheric light is pixel based. Mathematically,

$$\tilde{t}(x) = 1 - \min_{y \in \Omega(x)} \left(\min_{c} \left(\frac{I^c(x)}{\max_c(\mathrm{A}(x))} \right) \right) \tag{4.12}$$

4.5 Optimizing Transmission Refinement

In detail, halos occur in patches having regions of different depths i.e. the patches having depth discontinuities. Due to varying depths, the transmission of the farther region is over estimated. Since scene radiance J has an inverse relation with transmission, over estimation of transmission leads to whiteness all along the edges of those discontinuities.

Soft matting proposed by A. Levin et al. [15], has been used in the proposed algorithm to deal with halo effects. This step produces very good results as shown in the figure below.

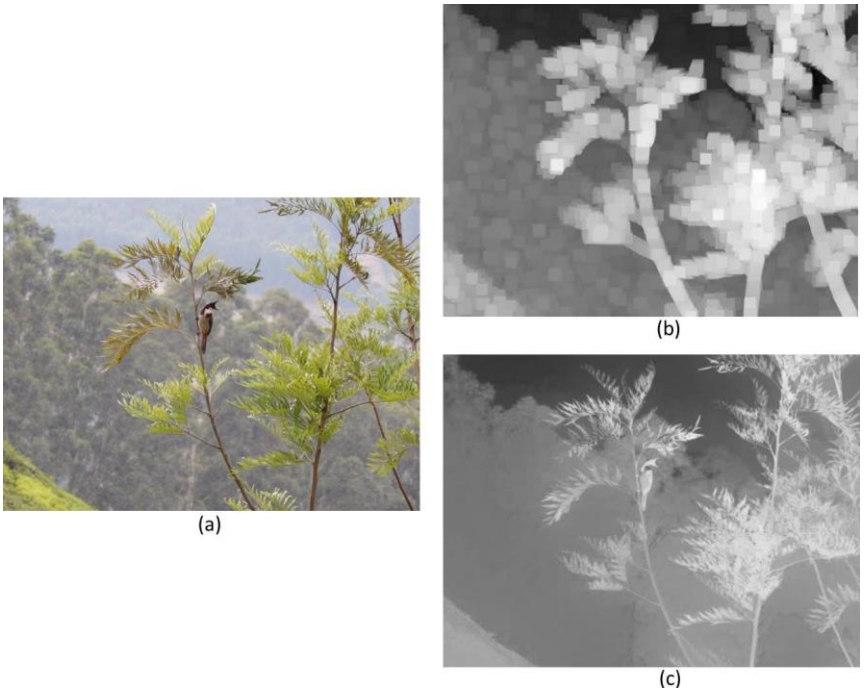

Figure 4.9: Transmission Refinement (a) Hazy image (b) Coarse transmission (c) Refined transmission

4.6 Scene Radiance Computation

After having calculated the atmospheric light and transmission, scene radiance can be calculated using haze imaging model with the only change of pixel based A.

$$J(x) = \left(\frac{I(x) - A(x)}{max(t(x), t_0)} \right) + A(x) \tag{4.13}$$

4.7 Proposed Algorithm

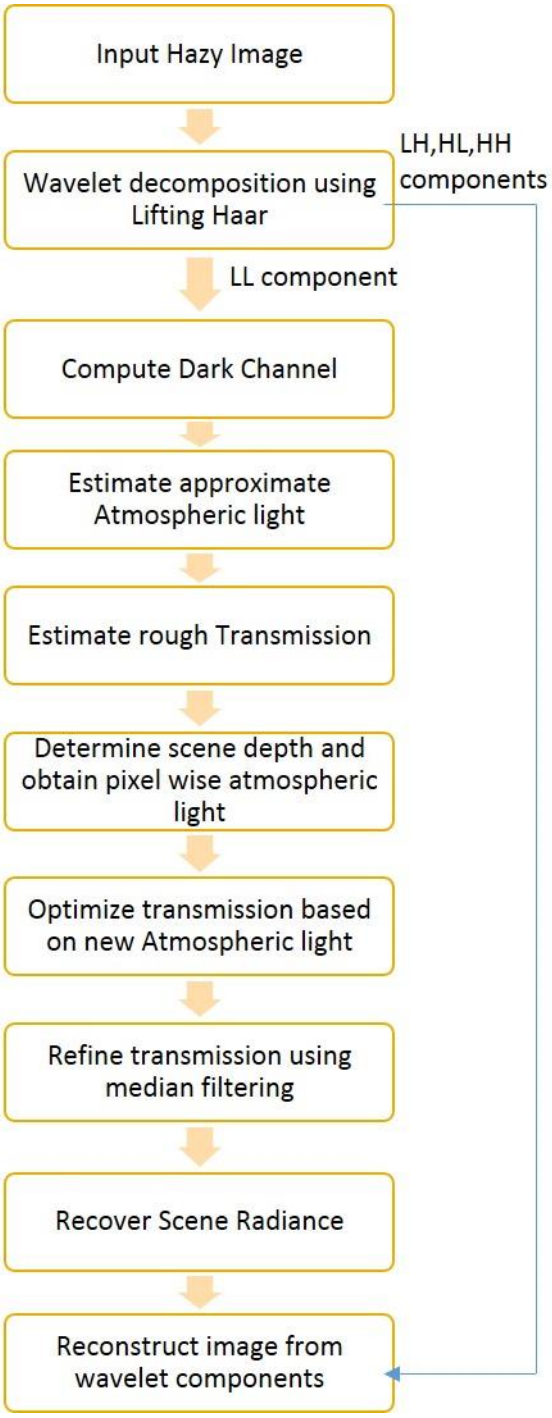

Figure 4.10 Algorithm Block Diagram

CHAPTER 5

SIMULATION AND RESULTS

In this section, we illustrate the efficacy of the proposed algorithm over a set of different types of real images. The haze free images obtained from our approach are compared with respective input hazy images and He's outputs. The performance of our algorithm is measured with two approaches:

1. Objective evaluation: where we check the run time of the algorithm critical for real time applications, Structural Similarity index (SSIM), entropy before and after dehazing algorithm and root mean square contras
2. Subjective evaluation: where we evaluate results on basis of visual inspection

Description of the simulation environment used for experimentation is Matlab-R2016a, Windows 7 professional (64bit), Intel core-i5 2.6 GHz (4CPUs), 4GB RAM.

5.1 Subjective Evaluation

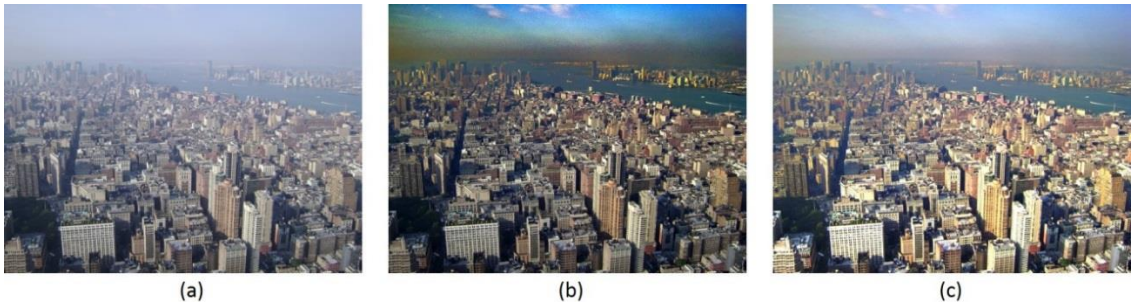

Figure 5.1: New York. Sky saturation problem (a) Hazy image (b) He's result (c) Our result

Figure 5.2: Mountain. Sky saturation problem (a) Hazy image (b) He's result (c) Our result

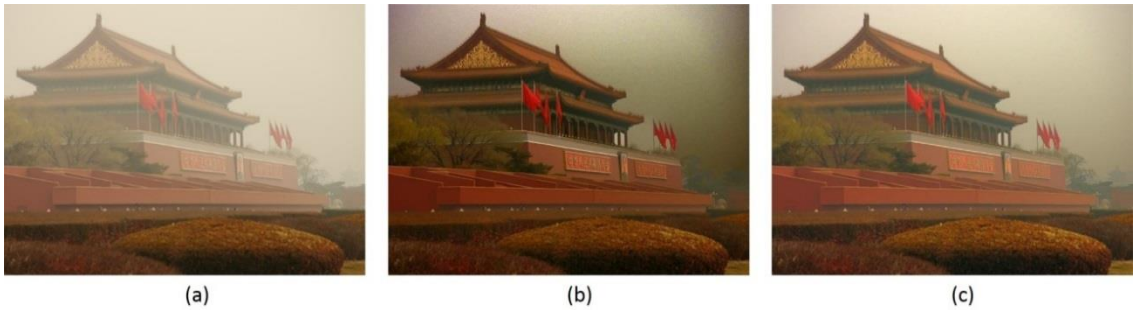

Figure 5.3: Temple. Sky saturation problem (a) Hazy image (b) He's result (c) Our result

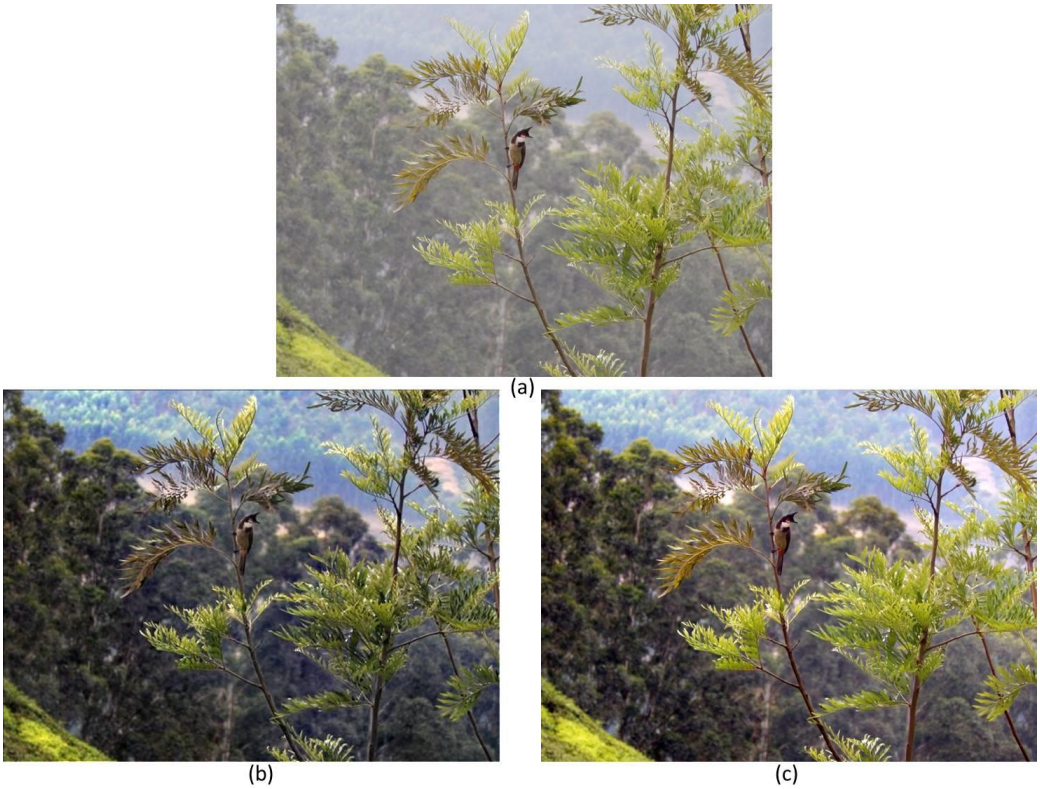

Figure 5.4: Bird. (a) Hazy image (b) He's result (c) Our result

Figure 5.5: Bird. Contrast and Color Fidelity Comparison (a) He's result (b) Our result

(a) (b) (c)

Figure 5.6: Canon. Contrast and Color Fidelity Comparison (a) He's result (b) Our result

(a) (b)

Figure 5.7:Canon. Contrast and Color Fidelity Comparison (a) He's result (b) Our result

(a) (b) (c)

Figure 5.8: Market. (a) He's result (b) Our result

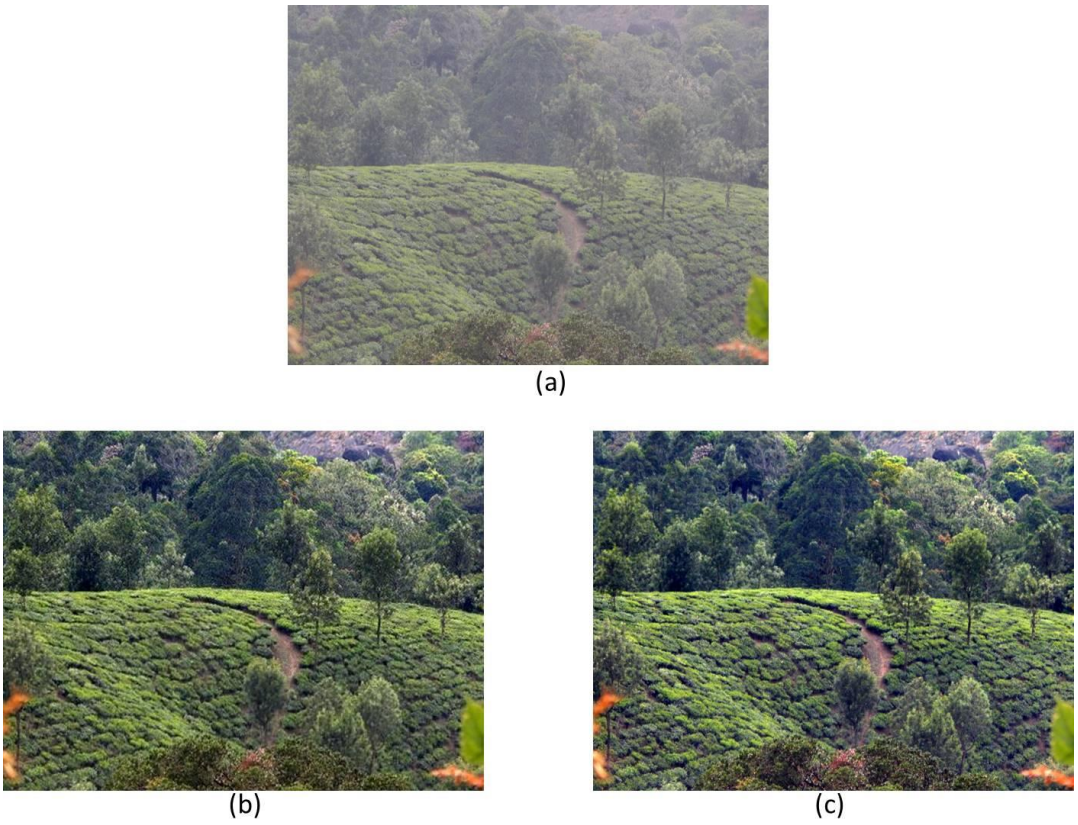

Figure 5.9: Tea Garden. Contrast and Brightness Comparison (a) Hazy image (b) He's result (c) Our result

In figure 5.1, on applying conventional DCP algorithm, sky is badly saturated while the output from our algorithm reproduces natural sky shades without compromising on the non-sky region. Same can be observed in figure 5.2 and 5.3 results.

In the next image showing a bird in grassland, natural colors are well preserved in our results which were otherwise lost using conventional method. This can be easily observed from the next zoomed in image focusing the red color on bird's tail. Despite color fidelity our results exhibit better contrast and brightness. Same can be noticed in figures 5.6 to 5.9.

5.2 Objective Evaluation

In the table below we show the run time comparison between our and He's algorithm. As can be seen, our algorithm far exceeds the conventional DCP in terms of speed.

Table 1: Run Time Comparison

Image name	Image Dimensions	He's method	Proposed method
New York	1024x768	117.723s	42.530s
Temple	600x450	29.042s	15.133s
Canon	400x600	46.307s	12.313s
Mountain	512x384	24.787s	10.890s
Bird	1152x864	162.504s	55.959s
Tea Garden	1152x864	161.940s	55.046s
Market	332x500	23.546s	9.491s

In order to quantify the image quality produced by our method in comparison to He's approach, we choose SSIM, entropy and contrast as performance parameters. Their physical significance to image dehazing along with formulation is as follows:

- **Structural Similarity Index**

  It indicates the degree of structure retained in a processed image with respect to reference image. In our case, we measure the structural similarity index of images produced from conventional DCP and the proposed technique considering hazy image as reference image. To measure SSIM we use the following formula:

$$SSIM(x,y) = \frac{(2\mu_x\mu_y + c_1)(2\sigma_{xy} + c_2)}{(\mu_x^2 + \mu_y^2 + c_1)(\sigma_x^2 + \sigma_y^2 + c_2)} \tag{5.1}$$

  As can be observed from the analysis table 2, haze free images produced from our method has higher values of SSIM than classical DCP technique

- **Contrast**

  Higher contrast makes it easy to differentiate among objects in an image. In present work, we use root mean square contrast as a metric. This is same as standard deviation. To measure rms contrast we use the following formula:

$$RMS\ Contrast = \sqrt{\frac{1}{MN}\sum_{i=0}^{N-1}\sum_{j=0}^{M-1}\left(I_{ij} - \bar{I}\right)^2} \tag{5.2}$$

  As can be easily observed from table 2, our method exceeds traditional technique in contrast as well.

- **Entropy**

  Entropy signifies randomness. Low value of entropy corresponds to homogenous regions of image. Since haze is distributed all over image, hazy image has low entropy as compared to haze free image. Thus, entropy can be somewhat related to amount of haze removed from the image. To measure entropy we use the following formula:

$$Entropy\ H = -\sum_{i} p_i(log_2 p_i) \tag{5.3}$$

  Our method once again outperforms the conventional DCP technique in terms of entropy as can be seen from the analysis table below.

In the table below we compare our prosed method with DCP on the basis of entropy and structural symmetry index. As can be observed that here also our algorithm performs better than the classic method in majority of cases.

Table 2: Parameter comparison

Parameter	*Entropy*			*SSIM*		*Contrast*		
Image	**Hazy image**	**Classical DCP**	**Proposed Algorithm**	**Classical DCP**	**Proposed Algorithm**	**Hazy image**	**Classical DCP**	**Proposed Algorithm**
Canon	6.89	7.23	7.2	0.58	0.66	6.28	6.02	5.66
Tea Garden	6.34	7.33	7.37	0.61	0.61	2.92	5.81	6.64
Bird	6.99	7.52	7.78	0.67	0.78	4.77	7.48	8.72
Market	7.3	7.84	7.89	0.61	0.65	6.74	9.44	10.07
Mountain	7.48	7.53	7.65	0.76	0.77	5.64	5.59	5.96
New York	7.61	7.64	7.77	0.7	0.78	7.69	7.67	8.88
Tiananmen	7.64	7.61	7.79	0.77	0.93	8.95	7.59	8.85

CHAPTER 6

CONCLUSION

In this thesis report, a novel single image dehazing method based on dark channel prior has been proposed. Atmospheric light is calculated for each pixel on the basis of its depth. This accurate estimation of airlight further leads to accuracy of transmission and scene radiance. The effectiveness of our method can be observed from the results produced. We do not require any additional correction factor or segmentation techniques to deal with sky region saturation; rather accurate estimation of atmospheric light enables the algorithm to implicitly retain natural sky shades. We used Haar lifting wavelet which made the algorithm fast and also simple and memory efficient.

CHAPTER 7

FUTURE WORK

In spite of much improvement over traditional DCP in our work, some common issue remains. Proposed algorithm still suffers from bluishness of scene area near the horizon as depicted below:

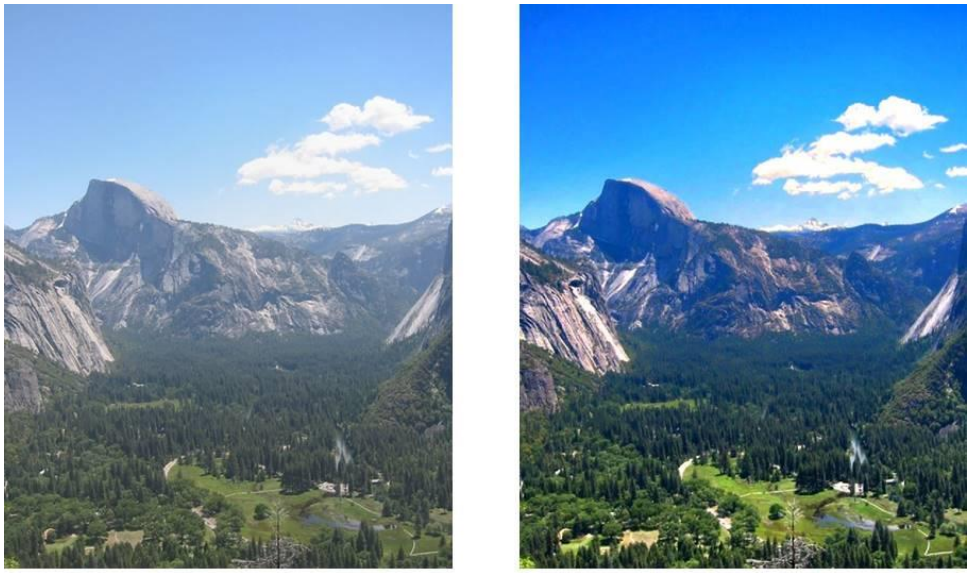

Figure 7.1: (a) hazy image, (b) output image with bluish problem

In future, we aim at taking our algorithm to the next level to overcome the above stated issue.

BIBLIOGRAPHY

1. Kaiming He, Jian Sun, and Xiaoou Tang, Fellow IEEE, “Single Image Haze Removal Using Dark Channel Prior”, *IEEE Transactions on Pattern Analysis and Machine Intelligence*, vol. 33, no. 12, December 2011
2. McCartney and Earl J., “Optics of the Atmosphere: Scattering by Molecules and Particles”, New York, *John Wiley and Sons*, Inc., 1976. 421 p. 1 (1976)
3. S. Narasimhan and S. Nayar, “Vision and the Atmosphere,” *International Journal on Computer Vision*, vol. 48, no. 3, Jul 2002, pp. 233–254
4. Yogesh Kumar, Jimmy Gautam, Ashutosh Gupta, Bhavin V. Kakani and Himansu Chaudhary, “Single Image Dehazing Using Improved Dark
5. Cheng-Hsiung Hsieh, Yu-Sheng Lin and Chih-Hui Chang, “Haze Removal Without Transmission Map Refinement Based On Dual Dark Channels”, *IEEE International Conference on Machine Learning and Cybernetics*, vol. 2, July 2014
6. Jiajie Liu, Jieying Zheng, Ziguan Cui, Guijin Tang and Feng Liu, “An Improved Image Dehazing Algorithm Based on Dark Channel Prior”, *IEEE Workshop on Advanced Research and Technology in Industry Applications (WARTIA),* September 2014
7. Chia-Hung Yeh, Li-Wei Kang, Cheng-Yang Lin and Chih-Yang Lin, “Efficient Image/Video Dehazing through Haze Density Analysis Based on Pixel-based Dark Channel Prior”, *IEEE Conference on Information Security and Intelligence Control (ISIC),* August 2012

   Channel Prior”, IEEE conference on Signal Processing and Integrated Networks (SPIN), February 2015

8. Xipan Lu, Guoyun Lv and Tao Lei, “Fast Single Image Dehazing Algorithm”, *IEEE Conference on Audio, Language and Image Processing (ICALIP)*, July 2014
9. Ting Han and Yi Wan, “A Fast Dark Channel Prior-based Depth Map Approximation Method for Dehazing Single Images”, IEEE Third International Conference on Information Science and Technology, March 2013
10. Hung-Yu Yang, Pei-Yin Chen, Chien-Chuan Huang, Ya-Zhu Zhuang, Yeu-Horng Shiau, “Low Complexity Underwater Image Enhancement Based on Dark Channel Prior”, *IEEE Conference on Innovations in Bio-inspired Computing and Applications (IBICA)*, December 2011
11. Yanjing Yang, Zhizhong Fu, Xinyu Li, Chang Shu and Xiaofeng Li, “A Novel Single Image Dehazing Method” , *IEEE International Conference on Computational Problem-solving (ICCP)*, October 2013
12. C. Chengtao, Z. Qiuyu and L. Yanhua, “Improved Dark Channel Prior Dehazing Approach Using Adaptive Factor”, *IEEE International Conference on Mechatronics and Automation (ICMA)*, August 2015
13. Robby T. Tan, “Visibility in Bad Weather from a Single Image”, *IEEE Computer Vision and Pattern Recognition*, 2008
14. Fattal, R., “Single Image Dehazing”, *ACM Transactions on Graphics*, 27(3), 721-729
15. Anat Levin, Dani Lischinski and Yair Weiss, “A Closed-Form Solution to Natural Image Matting”, *IEEE Transactions on Pattern Analysis and Machine Intelligence*, vol.30, no. 2, pp. 228-242, February 2008
16. W. Sweldens, "The Lifting Scheme: A Construction of second generation wavelets," SIAMJ. Math. Anal 1997
17. W. Sweldens, "The Lifting Scheme: A Custom Design construction of Biorthogonal," Wavelets Appl. Comput. Harmon. Anal. 3(2); 1996
18. I. Daubechies and W. Sweldens "Factoring wavelet transform into lifting steps" Technical report, Bell Laboratories, Lucent Technologies, 1996

19. W. Sweldens “Wavelets and the lifting scheme: A 5 minute tour“, ZAMM - Journal of Applied Mathematics and Mechanics, vol. 76 (Suppl. 2), pp. 41-44, 1996

APPENDIX A

Lifting Scheme Decomposition Steps

z-transform of discrete data sequence say $f(k)$ is

$$f(z) = \sum_k f(k) z^{-k} \tag{A.1}$$

On expanding:

$$f(z) = f(0)z^0 + f(1)z^{-1} + f(2)z^{-2} + f(3)z^{-3} + \cdots \tag{A.2}$$

$$f(-z) = f(0)z^0 - f(1)z^{-1} + f(2)z^{-2} - f(3)z^{-3} + \cdots \tag{A.3}$$

Adding above two:

$$\frac{f(z) + f(-z)}{2} = f(0)z^0 + f(2)z^{-2} + f(4)z^{-4} + \cdots = \sum_k f(2k) z^{-2k} \tag{A.4}$$

Sub-sampling $f(z)$ keeping even samples:

$$f_e(z) = \sum_k f(2k) z^{-k} \tag{A.5}$$

From (A.4) and (A.5):

$$f_e(z^2) = \frac{f(z) + f(-z)}{2} \tag{A.6}$$

In the same way, for odd samples,

$$f_o(z^2) = \left[\frac{f(z) - f(-z)}{2}\right] z \tag{A.7}$$

From (A.6) and (A.7),

$$f(z) = f_e(z^2) + z^{-1} f_o(z^2) \tag{A.8}$$

Upon low pass $h(z)$, and high pass $g(z)$ filtering of $f(z)$,

$$lp(z) = f(z)h(z) \tag{A.9}$$

$$hp(z) = f(z)g(z) \tag{A.10}$$

In matrix form:

$$\begin{bmatrix} lp(z) \\ hp(z) \end{bmatrix} = \begin{bmatrix} h(z) \\ g(z) \end{bmatrix} f(z) \tag{A.11}$$

Sub-sampling,

$$LP(z^2) = lp_e(z^2) = \frac{lp(z) + lp(-z)}{2} = \frac{h(z)f(z) + h(-z)f(-z)}{2} \quad \text{(A.12)}$$

$$HP(z^2) = hp_e(z^2) = \frac{hp(z) + hp(-z)}{2} = \frac{g(z)f(z) + g(-z)f(-z)}{2} \quad \text{(A.13)}$$

(A.12) and (A.13) in matrix form:

$$\begin{bmatrix} LP(z^2) \\ HP(z^2) \end{bmatrix} = \begin{bmatrix} lp_e(z^2) \\ hp_e(z^2) \end{bmatrix} = \frac{1}{2}\begin{bmatrix} h(-z) & h(z) \\ g(-z) & g(z) \end{bmatrix}\begin{bmatrix} f(-z) \\ f(z) \end{bmatrix} \quad \text{(A.14)}$$

Here, coefficients are calculated first and then subsampling is performed. This renders it highly inefficient. So to raise efficiency sub-sampling is performed before filtering,

$$lp_e(z) = [h(z)f(z)]_e = h_e(z)f_e(z) + z^{-1}h_o(z)f_o(z) \quad \text{(A.15)}$$

$$hp_e(z) = [g(z)f(z)]_e = g_e(z)f_e(z) + z^{-1}g_o(z)f_o(z) \quad \text{(A.16)}$$

Let output of sub-sampler and then low pass filter be $\lambda(z)$, and output of sub-sampler and then high pass filter be $\gamma(z)$

$$\begin{bmatrix} \lambda(z) \\ \gamma(z) \end{bmatrix} = P(z)\begin{bmatrix} f_e(z) \\ z^{-1}f_o(z) \end{bmatrix} \quad \text{(A.17)}$$

Where $P(z)$ is poly-phase matrix:

$$P(z) = \begin{bmatrix} h_e(z) & h_o(z) \\ g_e(z) & g_o(z) \end{bmatrix} \quad \text{(A.18)}$$

To ensure perfect reconstruction, low pass filter $h(z)$ and high pass filter $g(z)$ need to be complimentary, i.e. determinant of poly-phase matrix be unity:

$$P(z) = \begin{bmatrix} 1 & 0 \\ 0 & 1 \end{bmatrix} \tag{A.19}$$

New filter complimentary to g say h^{new} can be derived using primal lifting and new filter complimentary to h say g^{new} can be derived using dual lifting as:

$$h^{new} = h(z) + s(z^2)g(z) \tag{A.20}$$

$$g^{new} = g(z) + t(z^2)h(z) \tag{A.21}$$

(A.20) and (A.21) in poly-phase representation:

$$P^{new}(z) = \begin{bmatrix} h_e^{new}(z) & h_o^{new}(z) \\ g_e(z) & g_o(z) \end{bmatrix} = \begin{bmatrix} 1 & s(z) \\ 0 & 1 \end{bmatrix} \begin{bmatrix} h_e(z) & h_o(z) \\ g_e(z) & g_o(z) \end{bmatrix} \tag{A.22}$$

$$P^{new}(z) = \begin{bmatrix} h_e(z) & h_o(z) \\ g_e^{new}(z) & g_o^{new}(z) \end{bmatrix} = \begin{bmatrix} 1 & 0 \\ t(z) & 1 \end{bmatrix} \begin{bmatrix} h_e(z) & h_o(z) \\ g_e(z) & g_o(z) \end{bmatrix} \tag{A.23}$$

Poly-phase matrix can be written as product of upper and lower triangular matrices as:

$$P(z) = \begin{bmatrix} K1 & 0 \\ 0 & K2 \end{bmatrix} \prod_{i=m}^{1} \begin{bmatrix} 1 & s_i(z) \\ 0 & 1 \end{bmatrix} \begin{bmatrix} 1 & 0 \\ t_i(z) & 1 \end{bmatrix} \tag{A.24}$$

Factorizing $P(z)$ as:

$$P(z) = \begin{bmatrix} h_e(z) & h_o(z) \\ g_e(z) & g_o(z) \end{bmatrix} = \begin{bmatrix} h_e(z) & h_o^{new}(z) \\ g_e(z) & g_o^{new}(z) \end{bmatrix} \begin{bmatrix} 1 & s(z) \\ 0 & 1 \end{bmatrix} \tag{A.25}$$

That is

$$h_o(z) = s(z)h_e(z) + h_o^{new}(z) \tag{A.26}$$

$$g_o(z) = s(z)g_e(z) + g_o^{new}(z) \tag{A.27}$$

In the same way,

$$P(z) = \begin{bmatrix} h_e(z) & h_o(z) \\ g_e(z) & g_o(z) \end{bmatrix} = \begin{bmatrix} h_e^{new}(z) & h_o(z) \\ g_e^{new}(z) & g_o(z) \end{bmatrix} \begin{bmatrix} 1 & 0 \\ t(z) & 1 \end{bmatrix} \tag{A.28}$$

That is,

$$h_e(z) = h_e^{new}(z) + t(z)h_o(z) \tag{A.29}$$

$$g_e(z) = g_e^{new}(z) + s(z)g_o(z) \tag{A.30}$$